Available online at www.sciencedirect.com

SciVerse ScienceDirect

British Journal of Oral and Maxillofacial Surgery 52 (2014) 838–844

BRITISH Journal of Oral and Maxillofacial Surgery
www.bjoms.com

Evaluation of the potential of automatic segmentation of the mandibular canal using cone-beam computed tomography

Nicolaas Lucius Gerlach [a,b], Gerrit Jacobus Meijer [a,b,e], Dirk-Jan Kroon [c], Ewald Maria Bronkhorst [d], Stefaan Jozef Bergé [a,b], Thomas Jan Jaap Maal [a,b,*]

[a] *Department of Oral and Maxillofacial Surgery, Radboud University Nijmegen Medical Centre, Nijmegen, The Netherlands*
[b] *3D Facial Imaging Research Group Nijmegen, The Netherlands*
[c] *University of Twente, Signals and Systems Group, The Netherlands*
[d] *Department of Preventive and Curative Dentistry, Radboud University Nijmegen Medical Centre, Nijmegen, The Netherlands*
[e] *Department of Periodontology and Biomaterials, Radboud University Nijmegen Medical Centre, Nijmegen, The Netherlands*

Accepted 25 July 2014
Available online 22 August 2014

Abstract

We aimed to investigate the effectiveness of software for automatically tracing the mandibular canal on data from cone-beam computed tomography (CT). After the data had been collected from one dentate and one edentate fresh cadaver head, both a trained Active Shape Model (ASM) and an Active Appearance Model (AAM) were used to automatically segment the canals from the mandibular to the mental foramen. Semiautomatic segmentation was also evaluated by providing the models with manual annotations of the foramina. To find out if the tracings were in accordance with the actual anatomy, we compared the position of the automatic mandibular canal segmentations, as displayed on cross-sectional cone-beam CT views, with histological sections of exactly the same region. The significance of differences between results were analysed with the help of **Fisher's exact test and** Pearson's correlation coefficient. When tracings based on AAM and ASM were used, differences between cone-beam CT and histological measurements varied up to 3.45 mm and 4.44 mm, respectively. Manual marking of the mandibular and mental foramina did not improve the results, and there were no significant differences ($p = 0.097$) among the methods. The accuracy of automatic segmentation of the mandibular canal by the AAM and ASM methods is inadequate for use in clinical practice.

Keywords: Mandibular canal; automatic tracing; cadaver; cone-beam CT; 3-dimensional imaging

Introduction

Accurate preoperative planning is necessary to prevent iatrogenic damage to the neurovascular bundle that passes inside the mandibular canal, the course of which varies within the mandibular body.[1–4]

Three-dimensional,image-based, planning software gives us the opportunity to create a virtual mandibular canal.[5,6] Data from cone-beam computed tomography (CT) can be used. Until now tracing of the mandibular canal has been done manually and was time-consuming.[5] Several automatic methods of segmenting the mandibular canal have been published,[7–12] but only a few have concentrated on segmentation on cone-beam CT views.[11–13] Up to now the canal has been characterised by low contrast between it and the

* Corresponding author. Department of Oral and Maxillofacial Surgery 590, Radboud University Nijmegen Medical Centre, P.O. Box 9101, 6500 HB Nijmegen, The Netherlands. Tel.: +0031-243614550; fax: +0031-243541165.
E-mail address: T.Maal@mka.umcn.nl (T.J.J. Maal).

http://dx.doi.org/10.1016/j.bjoms.2014.07.253

surrounding tissues. [13]Areas with the same sort of tissue do not give the same amount of contrast because of the lack of uniformity of radiographic illumination and scattering.[13] As a consequence automatic segmentation of the canal is a challenge.

Obviously to prevent iatrogenic damage it is important that the position of the automatic tracing of the mandibular canal corresponds to its real anatomical position. None of the studies that have described automatic segmentation of the canal based on cone-beam CT data, have mentioned this.[11–13] To validate the results, automatic tracings have always been compared with manual tracings.[11–13] However, these are inaccurate and do not correspond to the real anatomical picture.[5]

The aim of this study was to assess the potential for automatic tracing of the mandibular canal as proposed by Kroon[13] using histological datasets as reference.

Material and Methods

To assess automatic tracings of the mandibular canal made from cone-beam CT data, the position of the canal as displayed on cross-sectional cone-beam CT images was compared with that of histological sections of the corresponding region. In one dentate and one edentate (Cawood and Howell classification V[14]) fresh frozen cadaver head, therefore, the second molar and second premolar region, both on the left and right sides of the mandible, were marked using titanium microscrews (5 mm long and 1.5 mm in diameter, KLS Martin, Gebrüder Martin GmbH&Co, Tuttlingen, Germany). These were positioned perpendicular to the mandibular arch at the free gingival margin in the vestibular fold.

To obtain cone-beam CT data, the skulls were scanned using the i-CAT™ 3-dimensional imaging system (Imaging Sciences International Inc, Hatfield, PA, USA) using the following **variables:** 120 kVp, 1.2 mA, 22 cm field of view, and 0.400 mm voxel size.[15,16]

To collect histological data, the mandibles were cut into small blocks and fixed in 4% neutral buffered formaldehyde. After dehydration in ethanol solutions from 70% to 100%, the samples were embedded in methylmethacrylate and cut into slices 10 μm thick in cross-sectional planes along the markers.[17] Methylene blue and basic fuchsin stains were used.

After the sections had been digitised into JPEG format using a Carl Zeiss light microscope and AxionVision Rel. 4.6 software (Carl Zeiss MicroImaging GmbH, Göttingen, Germany), distances from the middle of the canal to the outer surfaces of the mandibular body were measured (Adobe Photoshop CS4 Version 11.0; San Jose, California, USA). These measurements were used as reference values (A-D; Figure 1).

Different automatic methods of segmentation were investigated on the cone-beam CT data. The first was a modified Active Shape Model (ASM),[13,18] which included previous knowledge of the segmentation algorithm and variations

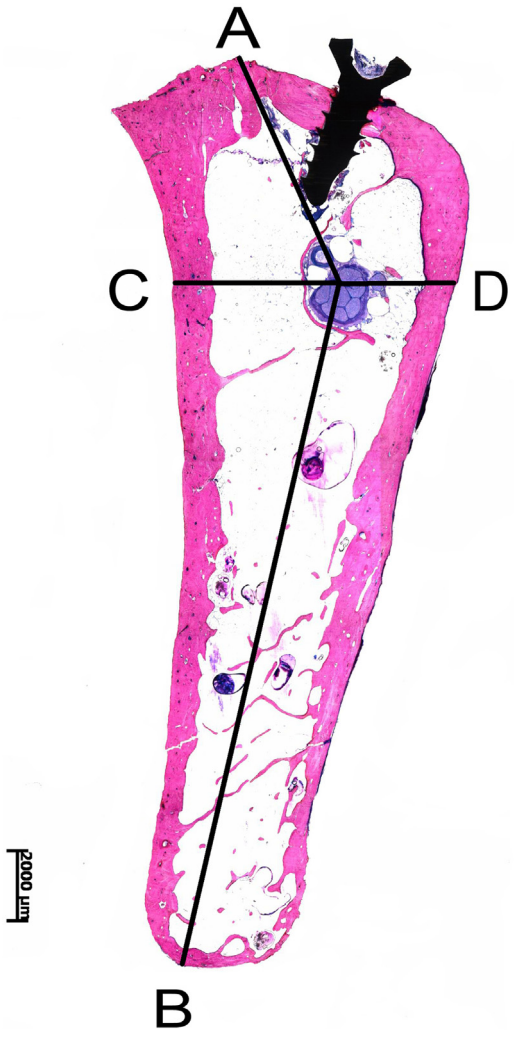

Figure 1. Distances measured on a histological section. The reference screw is clearly visible at the top. A = centre of the mandibular canal to the top of the alveolar ridge; B = centre of the mandibular canal to the base of the mandible; C = centre of the mandibular canal to the lingual surface; and D = centre of the mandibular canal to the buccal surface.

between corresponding points in training datasets, which were used as shape constraints during segmentation.[13,18]

The second method was the Active Appearance Model (AAM) segmentation procedure, which extended the ASM method, and not only included variations in shape but also data about appearance.[13,19] Both methods for tracing the canal automatically generated the mandibular foramen, the mental foramen, and the shape of the canal. They were used on expert segmentations of the mandibular canals and mandibles in 13 cone-beam CT datasets from both dentate and edentate patients.

Both the AAM and ASM based methods were expanded by providing them with manual annotations of the mandibular and mental foramena, which were marked by an experienced oral and maxillofacial surgeon. As a result only the course of the canal needed to be covered by automatic segmentation, and were referred to as AAM-$_{course}$ and ASM-$_{course}$.

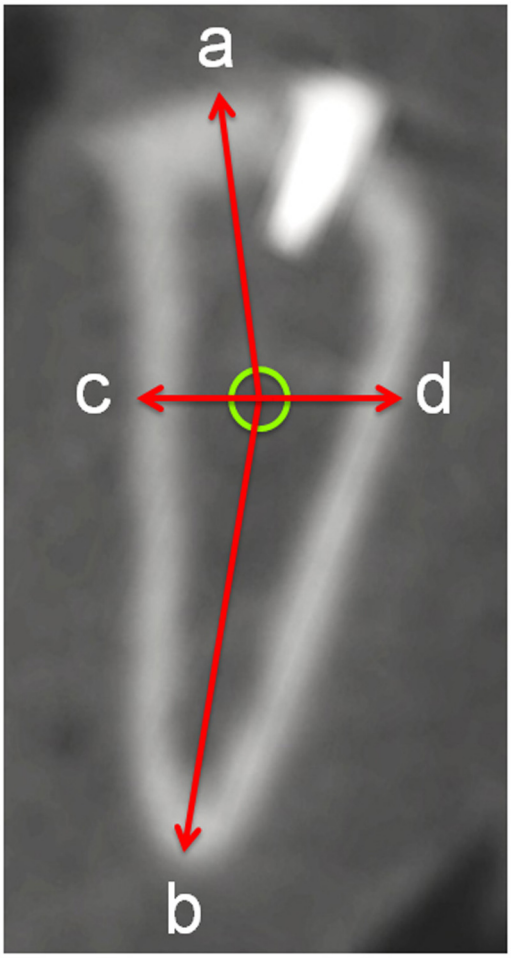

Figure 2. Example of a cross-sectional cone-beam computed tomographic (CT) view, showing the same region as Figure 1 (see the reference screw), and showing the corresponding measurements of the position of the mandibular canal (a, b, c, d).

To compare the results of the automatic tracings, data were imported into the planning software of Procera System (NobelClinician™, Nobel Biocare, Göteborg, Sweden). The same distances measured on the histological sections were compared with the measurements made on the corresponding cross-sectional cone-beam CT images (a-d; Figure 2). To establish the intra-observer variation, measurements were repeated 8 times with a time interval of 2 days.

The results are presented as mean (SD). In addition, differences between the cone-beam CT measurements and the histological measurements have been presented separately for the dentate and edentate jaws, and the significance of differences was analysed using Student's *t* test. As reported elsewhere, manual tracings of the canal can vary by up to 1.3 mm[5]. This threshold was therefore used to indicate whether the differences between cone-beam CT measurements and histological measurements were substantial. Fisher's exact test was used to assess the significance of differences between the methods. Pearson's correlation coefficient was calculated to quantify the relation, both in the dentate jaw and the edentate jaw, between various methods. Probabilities of less than 0.05 were accepted as significant.

Results

For each automatic method of tracing, AAM, ASM, $AAM_{-course}$ and $ASM_{-course}$ a total of 32 repeat measurements were made on the cone-beam CT views (8 sites, 4 distances). The results of the measurements on the cone-beam CT images and histological sections are shown in Tables 1 and 2. Both showed small ranges of distributions with SD ranging up to 0.41 mm in the dentate jaw and 0.22 mm in the edentate jaw.

Tables 3 and 4 show the differences between the position of the mandibular canal as dictated by the automatic software on the cone-beam CT images compared with the position of the canal on the corresponding histological sections.

When the AAM method was used, distances ranged from 3.45 mm smaller to 3.27 mm larger. When the ASM measurements were used, these differences ranged from minus or plus 4.44 mm. Manual annotation of the mandibular and mental foramena resulted in maximum differences of 5.60 mm below to 3.90 mm above the mean when the $AAM_{-course}$ method was used, and ranged from 4.35 mm below to 5.11 mm above the mean. Confidence intervals showed that all comparisons, except 5 of the dentate samples in the the $ASM_{-course}$ group, were significant ($p = 0.0001$).

When the differences between the dentate and edentate measurements using the AAM method were analysed, Pearson's correlation coefficient was 0.67, indicating good agreement. When the ASM method was used, this correlation was even higher at 0.84. However, the correlations for the $AAM_{-course}$ and $ASM_{-course}$ methods were rather low (0.32 and 0.35).

The difference between cone-beam CT measurements and histological measurements of more than 1.3 mm was substantial. Of 32 repeat measurements AAM = 20, ASM = 22, and $AAM_{-course}$ and $ASM_{-course}$ = 14 each, values were outside this threshold. These counts did not differ significantly ($p = 0.097$).

Discussion

Automatic tracing of the mandibular canal can provide advantages over manual tracing, as it might be more accurate and save time. However, our results show that it is still not accurate enough.

We know of few studies that have addressed the automatic tracing of the mandibular canal on cone-beam CT data.[11–13] Kainmuller et al.[11] described an ASM that segmented both the mandibular body and the canal. A Dijkstra-based procedure was applied for fine-tuning. This algorithm calculates the shortest path between the different dark points in the canal.[13] Training comprised 106 manually segmented

Table 1
Mean (SD) dentate measurements (mm) of the position of the mandibular canal based on cone-beam CT images and the reference distances based on histological measurements.

Dentate site	Dentate distance	AAM	ASM	AAM-course	ASM-course	Histology
1	A	17.89 (0.08)	20.01 (0.11)	18.28 (0.15)	20.60 (0.15)	16.69 (0.13)
2	A	21.29 (0.19)	21.28 (0.17)	20.18 (0.10)	19.54 (0.11)	19.00 (0.19)
3	A	22.70 (0.12)	22.65 (0.21)	18.36 90.41)	19.91 (0.15)	20.34 (0.09)
4	A	18.36 (0.09)	20.89 (0.16)	16.68 (0.18)	21.55 (0.09)	16.45 (0.09)
1	B	11.15 (0.09)	8.89 (0.08)	11.10 (0.14)	8.80 (0.11)	12.86 (0.34)
2	B	9.41 (0.10)	9.26 (0.15)	10.78 (0.07)	11.85 (0.09)	11.55 (0.27)
3	B	8.40 (0.09)	8.71 (0.16)	12.09 (0.18)	11.10 (0.12)	11.56 (0.24)
4	B	12.54 (0.09)	10.28 (0.09)	13.98 (0.13)	9.23 (0.09)	13.58 (0.12)
1	C	4.28 (0.09)	2.19 (0.10)	2.81 (0.10)	2.30 (0.11)	2.05 (0.08)
2	C	4.94 (0.14)	3.71 (0.16)	5.88 (0.12)	6.19 (0.08)	6.15 (0.11)
3	C	3.85 (0.05)	4.48 (0.09)	5.73 (0.20)	5.48 (0.10)	6.70 (0.12)
4	C	2.56 (0.07)	2.33 (0.10)	1.85 (0.13)	2.16 (0.07)	1.49 (0.09)
1	D	4.33 (0.10)	5.24 (0.12)	5.80 (0.09)	5.31 (0.18)	5.45 (0.11)
2	D	3.38 (0.10)	4.81 (0.12)	2.48 (0.09)	1.91 (0.08)	1.96 (0.13)
3	D	4.65 (0.09)	3.90 (0.09)	2.41 (0.17)	1.94 (0.21)	2.05 (0.06)
4	D	4.65 (0.08)	4.41 (0.11)	6.60 (0.13)	4.35 (0.13)	4.26 (0.12)

AAM = active appearance model, and ASM = active shape model.

datasets. The mean distance compared with manual annotation of the mandibular canal was 1.0 (0.6) mm for the right canal and 1.2 (0.9) mm for the left canal.[11]

To obtain the mandibular and mental foramena Kim et al.[12] described an automatic method using 3-dimensional rendering of the panoramic volume and analysis of the texture. In a next step, a Dijkstra's algorithm was used to segment the canal, and was tested on 10 cone-beam CT datasets. Again, manual tracings of the canal were the gold standard. The mean (SD) distance to expert segmentation was 0.73 mm (0.69) mm.[12]

Several more methods can be used to localise and segment the mandibular canal automatically, and Kroon[13] modified and analysed them for use with cone-beam CT data. He tested the performances of the Lucas Kanade template tracking method,[20] the Basis spline registration method,[21] and the demon registration method,[22] and compared these with the AAM and ASM methods, before concluding that the AAM and ASM methods were best (which is why we chose them for the current study).

These models were used on 13 cone-beam CT datasets in which the mandibular canal was annotated by an experienced

Table 2
Mean (SD) dentate measurements (mm) of the position of the mandibular canal based on cone-beam CT images and the reference distances based on histological measurements.

Edentate site	Edentate distance	AAM	ASM	AAM-course	ASM-course	Histology
1	A	8.80 (0.15)	8.68 (0.10)	11.10 (0.12)	8.40 (0.08)	7.20 (0.13)
2	A	6.20 (0.11)	6.29 (0.11)	5.74 (0.11)	6.53 (0.10)	2.93 (0.05)
3	A	5.69 (0.11)	5.71 (0.08)	7.08 (0.12)	6.10 (0.17)	4.23 (0.06)
4	A	7.13 (0.07)	9.65 (0.12)	9.91 (0.14)	7.29 (0.14)	6.70 (0.04)
1	B	18.14 (0.07)	17.54 (0.07)	1.,73 (0.10)	18.39 (0.08)	20.32 (0.11)
2	B	6.33 (0.13)	6.45 (0.12)	7.49 (0.10)	6.34 (0.12)	9.78 (0.03)
3	B	8.21 (0.06)	7.81 (0.12)	7.04 (0.12)	7.59 (0.10)	9.10 (0.06)
4	B	10.65 (0.12)	7.86 (0.15)	8.70 (0.09)	10.63 (0.16)	12.30 (0.05)
1	C	5.16 (0.12)	3.71 (0.11)	3.83 (0.07)	4.11 (0.11)	4.89 (0.06)
2	C	3.79 (0.12)	3.73 (0.09)	4.73 (0.09)	3.09 (0.10)	3.36 (0.04)
3	C	4.50 (0.09)	4.40 (0.08)	4.96 (0.14)	3.75 (0.11)	5.12 (0.13)
4	C	2.45 (0.13)	4.14 (0.05)	3.99 (0.11)	4.11 (0.08)	4.43 (0.05)
1	D	3.01 (0.08)	4.99 (0.20)	3.91 (0.08)	4.76 (0.11)	3.26 (0.07)
2	D	5.40 (0.09)	5.28 (0.10)	5.21 (0.10)	5.95 (0.12)	2.74 (0.05)
3	D	4.25 (0.05)	4.49 (0.06)	4.00 (0.09)	5.41 (0.08)	2.80 (0.22)
4	D	6.21 (0.14)	4.45 (0.12)	4.96 (0.05)	4.84 (0.18)	4.65 (0.06)

AAM = active appearance model, and ASM = active shape model.

Table 3
Overview of the difference (mean and 95% CI, mm) between the position of the mandibular canal when 4 different methods of tracing the mandibular canal were compared with histological sections of the corresponding cone-beam CT sites in the dentate jaw.

Dentate site	Dentate distance	AAM		ASM		AAM-$_{course}$		ASM-$_{course}$	
1	A	1.20	(1.09 to 1.31)	3.32	(3.20 to 3.45)	1.59	(1.45 to 1.73)	3.91	(3.77 to 4.05)
2	A	2.29	(2.10 to 2.48)	2.28	(2.10 to 2.46)	1.18	(1.03 to 1.33)	0.54	(0.39 to 0.70)
3	A	2.36	(2.25 to 2.47)	2.31	(2.15 to 2.47)	−1.98	(−2.27 to −1.68)	−0.43	(−0.55 to −0.31)
4	A	1.92	(1.83 to 2.01)	4.44	(4.31 to 4.58)	0.23	(0.09 to 0.37)	5.11	(5.02 to 5.20)
1	B	−1.71	(−1.96 to −1.46)	−3.97	(−4.22 to −3.72)	−1.76	(−2.02 to −1.50)	−4.06	(−4.31 to −3.81)
2	B	−2.14	(−2.34 to −1.94)	−2.29	(−2.51 to −2.07)	−0.78	(−0.97 to −0.58)	0.30	(0.10 to 0.50)
3	B	−3.16	(−3.34 to −2.98)	−2.85	(−3.05 to −2.65)	0.53	(0.32 to 0.74)	−0.46	(−0.65 to −0.28)
4	B	−1.04	(−1.14 to −0.93)	−3.30	(−3.41 to −3.20)	0.40	(0.28 to 0.52)	−4.35	(−4.46 to −4.25)
1	C	2.23	(2.14 to 2.31)	0.14	(0.05 to 0.23)	0.77	(0.68 to 0.86)	0.25	(0.16 to 0.35)
2	C	−1.21	(−1.33 to −1.09)	−2.44	(−2.57 to −2.30)	−0.27	(−0.38 to −0.16)	0.04	(−0.06 to 0.14)
3	C	−2.85	(−2.94 to −2.76)	−2.23	(−2.33 to −2.12)	−0.98	(−1.14 to −0.82)	−1.23	(−1.34 to −1.12)
4	C	1.08	(0.99 to 1.16)	0.84	(0.74 to 0.94)	0.36	(0.25 to 0.48)	0.68	(0.59 to 0.76)
1	D	−1.12	(−1.23 to −1.02)	−0.21	(−0.33 to −0.10)	0.35	(0.25 to 0.45)	−0.14	(−0.29 to 0.01)
2	D	1.41	(1.30 to 1.53)	2.85	(2.72 to 2.98)	0.51	(0.40 to 0.62)	−0.05	(−0.16 to 0.06)
3	D	2.60	(2.52 to 2.68)	1.85	(1.77 to 1.93)	0.36	(0.23 to 0.49)	−0.11	(−0.27 to 0.04)
4	D	0.39	(0.29 to 0.49)	0.15	(0.04 to 0.27)	2.34	(2.22 to 2.46)	0.09	(−0.04 to 0.21)

AAM = active appearance model, and ASM = active shape model.

oral and maxillofacial surgeon.[13] These manual tracings were also used for validation. The mean (SD) deviations from manual annotation using the modified AAM and ASM methods were 1.99 (0.70) mm and 2.27 (0.69) mm, respectively. Kroon[13] has already proposed more investigations to improve these results.

Because datasets were segmented manually, the results of these studies are hard to interpret and cannot be compared with our results.[11–13] Obviously, it is important to know the exact position of the mandibular canal preoperatively, and this may differ from a manually- assigned position based on cone-beam CT. We have therefore compared the automatically segmented canals with their anatomical position on histological slides as a reference.

Although we found no significant differences between the AAM and ASM methods of segmentation (with mean differences up to 3.45 mm between the histological and the automatic methods of segmentation) the AAM is better than

Table 4
Overview of the difference (mean and 95% CI, mm) between the position of the mandibular canal when 4 different methods of tracing the mandibular canal were compared with histological sections of the corresponding cone-beam CT sites in the edentate jaw.

Edentate site	Edentate distance	AAM		ASM		AAM-$_{course}$		ASM-$_{course}$	
1	A	1.60	(1.46 to 1.74)	1.47	(1.35 to 1.59)	3.90	(3.77 to 4.02)	1.20	(1.09 to 1.30)
2	A	3.27	(3.19 to 3.35)	3.36	(3.27 to 3.45)	2.81	(2.73 to 2.89)	3.60	(3.52 to 3.68)
3	A	1.46	(1.37 to 1.55)	1.49	(1.41 to 1.56)	2.85	(2.75 to 2.94)	1.87	(1.75 to 2.00)
4	A	0.42	(0.37 to 0.48)	2.95	(2.86 to 3.04)	3.21	(3.11 to 3.31)	0.59	(0.49 to 0.69)
1	B	−2.19	(−2.28 to −2.09)	−2.79	(−2.88 to −2.69)	−5.60	(−5.70 to −5.49)	−1.94	(−2.03 to −1.84)
2	B	−3.45	(−3.54 to −3.36)	−3.33	(−3.41 to −3.24)	−2.29	(−2.36 to −2.22)	−3.44	(−3.52 to −3.35)
3	B	−0.88	(−0.95 to −0.82)	−1.28	(−1.38 to −1.19)	−2.06	(−2.15 to −1.97)	−1.51	(−1.59 to −1.43)
4	B	−1.65	(−1.74 to −1.56)	−4.44	(−4.55 to −4.33)	−3.60	(−3.68 to −3.53)	−1.68	(−1.79 to −1.56)
1	C	0.27	(0.18 to 0.37)	−1.18	(−1.27 to −1.09)	−1.06	(−1.13 to −1.00)	−0.78	(−0.87 to −0.69)
2	C	0.42	(0.33 to 0.52)	0.36	(0.29 to 0.43)	1.36	(1.29 to 1.43)	−0.28	(−0.35 to −0.20)
3	C	−0.62	(−0.73 to −0.51)	−0.72	(−0.83 to −0.62)	−0.16	(−0.29 to −0.02)	−1.37	(−1.49 to −1.25)
4	C	−1.98	(−2.08 to −1.88)	−0.29	(−0.34 to −0.24)	−0.44	(−0.53 to −0.35)	−0.32	(−0.39 to −0.25)
1	D	−0.25	(−0.33 to −0.17)	1.73	(1.58 to 1.87)	0.65	(0.57 to 0.73)	1.50	(1.41 to 1.59)
2	D	2.66	(2.59 to 2.74)	2.54	(2.46 to 2.62)	2.47	(2.40 to 2.55)	3.21	(3.12 to 3.30)
3	D	1.45	(1.30 to 1.61)	1.69	(1.53 to 1.85)	1.20	(1.04 to 1.37)	2.62	(2.45 to 2.78)
4	D	1.56	(1.46 to 1.67)	−0.20	(−0.30 to −0.11)	0.31	(0.25 to 0.37)	0.19	(0.05 to 0.32)

AAM = active appearance model, and ASM = active shape model.

the ASM method. The ASM method learns the variations in shape from training datasets, assuming a Gaussian distribution of shapes between subjects. Because the number of training datasets is limited to 13, this Gaussian assumption might not be valid, which probably explains the large differences between the actual position of the mandibular canals and the position given by automatic segmentation.

The methods AAM-$_{course}$ and ASM-$_{course}$ were introduced to try to find out if the automatic segmentation of the methods based on the AAM and ASM methods were improved by the addition of manual annotations of both the mandibular and mental foramena. Surprisingly, differences between the AAM/ASM-$_{course}$ segmentation and histological sections were even larger (up to 5.60 mm). Apparently, as the variations in shape of the canals are limited because there are so few training datasets and, when the starting point and end point of the automatic segmentations are fixed, larger differences in the remaining course of the canal are the result.

An automatic method of segmenting the canal should equalise or even be better than manual tracings. The methods proposed by Kroon[13] do not meet this standard. In two-thirds of the comparisons manual tracings of the canal were better than those automatically segmented.

The accuracy of manually marked tracings of the mandibular canal depends on the presence of teeth, resulting in more disturbances on cone-beam CT images, and therefore an increase in errors of measurement,[16] which is why we included both a dentate and an edentate cadaver. Although differences between the histological and the cone-beam CT measurements with both the AAM and ASM methods show similar patterns for the dentate and the edentate distances, correlation between the dentate and edentate measurements when the AAM-$_{course}$ and ASM-$_{course}$ methods were used was low, indicating that teeth had no effect on the outcome. Methods based on AAM and ASM, preceded by manual notation of the mandibular and mental foramena, apparently result in more random tracings and do not improve accuracy.

Two cadavers were measured at each of 4 sites, and deviations in manual tracings of the mandibular canal increase, particularly towards the mental foramen.[5] Although the anterior sections are positioned in the second premolar region (the region of the anterior loop) the effect of automatic tracing of the mandibular canal in this region remained unclear. Our sample size was small, and because the study was designed to test the potential of methods of automatic tracing, this was acceptable. When differences between histological and cone-beam CT sections are reduced as a result of improvements of the methods of automatic tracing, further research with larger samples and analysis of the whole canal will be needed.

The success of the segmentations is highly dependent on the quality of the images acquired by the cone-beam CT scanner. There are many scanners commercially available, so the type of scanner, the technique of scanning, and the resolution may influence the success of the algorithms. The iCat scanner, configured with a low-resolution protocol, is used daily in our hospital and we therefore used it in this study. Results might be better with a different type of scanner and different scanning protocols.

Training datasets that comprise human cadavers, in which the true anatomical position of the course of the canal is established, are obligatory to develop accurate automatic tracing algorithms for the mandibular canal based on previous knowledge. In this way human inaccuracy during manual tracing can be excluded. In the next study it will be important to increase the number of heads to deliver proper validation data that are relevant to clinicians.

In conclusion, we found no significant differences in automatic tracing of the mandibular canal between the AAM, ASM, AAM-$_{course}$, and ASM-$_{course}$ methods. Differences between these methods and the true anatomical position of the mandibular canal are still substantial. Further training and validation on human cadavers are needed to optimise methods of automatic tracing of the mandibular canal.

Conflict of Interest

We have no conflict of interest.

Ethics statement/confirmation of patients' permission

Not necessary.

Acknowledgements

The authors thank the Department of Anatomy and the Department of Biomaterials, Radboud University Nijmegen, Medical Centre, The Netherlands for providing the human cadaver heads and preparing the histological specimen. We thank O.H.H. Gerlach for editing this manuscript.

This project was funded by Nobel Biocare. The funders had no role in study design, collection and analysis of data, preparation of the manuscript or in the decision to submit for publication.

References

1. Anderson LC, Kosinski TF, Mentag PJ. A review of the intraosseous course of the nerves of the mandible. *J Oral Implantol* 1991;**17**:394–403.
2. Hwang K, Lee WJ, Song YB, et al. Vulnerability of the inferior alveolar nerve and mental nerve during genioplasty: an anatomic study. *J Craniofac Surg* 2005;**16**:10–4.
3. Kieser J, Kieser D, Hauman T. The course and distribution of the inferior alveolar nerve in the edentulous mandible. *J Craniofac Surg* 2005;**16**:6–9.
4. Uchida Y, Yamashita Y, Goto M, et al. Measurement of anterior loop length for the mandibular canal and diameter of the mandibular incisive canal to avoid nerve damage when installing endosseous implants in the interforaminal region. *J Oral Maxillofac Surg* 2007;**65**:1772–9.

5. Gerlach NL, Meijer GJ, Maal TJ, et al. Reproducibility of 3 different tracing methods based on cone beam computed tomography in determining the anatomical position of the mandibular canal. *J Oral Maxillofac Surg* 2010;**68**:811–7.
6. Ghaeminia H, Meijer GJ, Soehardi A, et al. Position of the impacted third molar in relation to the mandibular canal. Diagnostic accuracy of cone beam computed tomography compared with panoramic radiography. *Int J Oral Maxillofac Surg* 2009;**38**:964–71.
7. Stein W, Hassfeld S, Muhling J. Tracing of thin tubular structures in computer tomographic data. *Comput Aided Surg* 1998;**3**:83–8.
8. Kondo T, Ong SH, Foong KW. Computer-based extraction of the inferior alveolar nerve canal in 3-D space. *Comput Methods Programs Biomed* 2004;**76**:181–91.
9. Rueda S, Gil JA, Pichery R, et al. Automatic segmentation of jaw tissues in CT using active appearance models and semi-automatic landmarking. *Med Image Comput Comput Assist Interv* 2006;**9**:167–74.
10. Yau H, Lin Y, Tsou L, et al. An adaptive region growing method to segment inferior alveolar nerve canal from 3D medical images for dental implant surgery. *Computer-Aided Design and Applications* 2008;**5**:743–52.
11. Kainmueller D, Lamecker H, Seim H, et al. Automatic extraction of mandibular nerve and bone from cone-beam CT data. *Med Image Comput Comput Assist Interv* 2009;**12**:76–83.
12. Kim G, Lee J, Lee H, et al. Automatic extraction of inferior alveolar nerve canal using feature-enhancing panoramic volume rendering. *IEEE Trans Biomed Eng* 2011;**58**:253–64.
13. Kroon DJ. *Segmentation of the mandibular canal in cone-beam CT data*. Gildeprint BV: Enschede; 2011.
14. Cawood JI, Howell RA. A classification of the edentulous jaws. *Int J Oral Maxillofac Surg* 1988;**17**:232.
15. Gerlach NL, Meijer GJ, Borstlap WA, et al. Accuracy of bone surface size and cortical layer thickness measurements using cone beam computerized tomography. *Clin Oral Implants Res* 2013;**24**:793–7.
16. Gerlach NL, Ghaeminia H, Bronkhorst EM, et al. Accuracy of assessing the mandibular canal on cone-beam computed tomography: a validation study. *J Oral Maxillofac Surg* 2014;**72**:666–71.
17. Van der Lubbe HB, Klein CP, De Groot K. A simple method for preparing thin (10 microM) histological sections of undecalcified plastic embedded bone with implants. *Stain Technol* 1988;**63**:171–6.
18. Cootes TF, Taylor CJ, Cooper D, et al. Active shape models, their training and application. *Computer Vision and Image Understanding* 1995;**61**:38–59.
19. Cootes TF, Edwards GJ, Taylor CJ. Active appearance models. In: Burkhardt H, Neumann B, eds. *Proceedings of the European Conference on Computer Vision* 1998; 2:484-98.
20. Baker S, Gross R, Matthews I. Lucas-Kanade 20 years on: a unifying framework. *International Journal of Computer Vision* 2004;**56**:221–55.
21. Rueckert D, Sonoda L, Hayes C, et al. Non-rigid registration using free-form deformations: application to breast MR images. *IEEE Transactions Med Imaging* 1999;**8**:712–21.
22. Thirion J. Image matching as a diffusion process: an analogy with Maxwell's demons. *Med Image Anal* 1998;**2**:243–60.